FILE

Institute of
Oceanographic Sciences
Deacon Laboratory

INTERNAL DOCUMENT No. 293

Initial results from a fine resolution model of the Southern Ocean

D J Webb, B A De Cuevas, P D Killworth &
M Rowe

1990

Natural Environment Research Council

INSTITUTE OF OCEANOGRAPHIC SCIENCES
DEACON LABORATORY

INTERNAL DOCUMENT No. 293

Initial results from a fine resolution model of the Southern Ocean

D J Webb, B A De Cuevas, P D Killworth & M Rowe

1990

Wormley
Godalming
Surrey GU8 5UB
Tel 0428 684141
Telex 858833 OCEANS G
Telefax 0428 683066

DOCUMENT DATA SHEET

AUTHOR
WEBB, D.J., CUEVAS, B.A. de, KILLWORTH, P.D. & ROWE, M.

PUBLICATION DATE 1990

TITLE

Initial results from a fine resolution model of the Southern Ocean.

REFERENCE

Institute of Oceanographic Sciences Deacon Laboratory, Internal Document, No. 293, 10pp. & figs. (Unpublished manuscript)

ABSTRACT

We have carried out a numerical integration of an eddy-resolving model of the Southern Ocean as part of a UK Project to improve the ocean models used for climate prediction. For the first six years of integration the model was spun up using a long timescale robust diagnostic method. The resulting temperature, salinity and velocity fields are in good qualitative agreement with available observations. The model results show that the Circumpolar Current contains embedded high velocity filaments which follow the bottom topography of the ocean. One filament passing through the Udintsev Fracture Zone in the South Pacific, transports 100 x 10^6 m^3 s^{-1} through a channel less than 130 km wide. The model reproduces the eddies formed by the Agulhas Current and shows that these transport 0.2 PW of heat from the Indian Ocean into the Atlantic Ocean.

KEYWORDS

AGULHAS CURRENT
ANTARCTIC
ANTARCTIC CIRCUMPOLAR CURRENT
BRAZIL CURRENT
DRAKE PASSAGE
EAST AUSTRALIAN CURRENT
MATHEMATICAL MODELLING
OCEAN EDDIES
OCEAN MODEL
ROSS SEA
SOUTHERN OCEAN
WEDDELL SEA

ISSUING ORGANISATION

Institute of Oceanographic Sciences
Deacon Laboratory
Wormley, Godalming
Surrey GU8 5UB. UK.

Director: Colin Summerhayes DSc

Telephone Wormley (0428) 684141
Telex 858833 OCEANS G.
Facsimile (0428) 683066

Copies of this report are available from: **The Library,** *PRICE* £00.00

Existing numerical models of the Southern Ocean, like those utilised for climate prediction, use a model grid with a horizontal resolution of 100 km or more. This is too coarse to correctly represent either the major ocean currents (the Gulf Stream is typically 50 km wide) or the oceanic eddy field (eddies of 100-200 km diameter). The models are not good at reproducing detailed field observations and they may not be adequate for good climate prediction. Although the computer costs are high, models which can resolve these features should provide a substantial improvement in realism, be better for predicting climate change and also provide better insight into the physics controlling the ocean.

The eddy-resolving model used for the present study is based on that of Cox (1984), with 32 vertical levels and a horizontal grid spacing of 1/2° in the east-west direction and 1/4° north-south. The model uses viscosity coefficients of 2×10^2 m^2s^{-1} horizontally and 10^{-4} m^2s^{-1} vertically. The diffusion coefficients for temperature and salinity are 10^2 m^2s^{-1} horizontally and 10^{-4} m^2s^{-1} vertically. The topography is based on the DBDB5 depth data set (U.S. Naval Oceanographic Office), smoothed to a one-degree grid to prevent topographic instabilities (Killworth, 1987). Linear bottom friction is used, corresponding to an e-folding time of 50 days for a 4000 m ocean. The boundary condition used at the northern open boundary is that proposed by Stevens (1990).

The model was first initialised using the Levitus (1982) temperature and salinity fields (this is a smoothed data set based on field measurements), and zero velocity. This method was found to be unstable due to barotropic modes trapped near Kerguelen and New Zealand driven by the interaction between bottom pressure and topography. The system was reinitialised as a cold (-2°C), saline ($36.69^{o}/_{oo}$), motionless fluid, and the temperature and salinity fields then dynamically relaxed to the Levitus data. During the first 2 years 160 days, the relaxation timescale used is 180 days for the top 140 m and 540 days for the deeper levels. From then up to six years the timescale is 360 days throughout. This is equivalent to the normal robust diagnostic scheme (Sarmiento and Bryan, 1982), except that the relaxation is so weak that it permits eddies, fronts, and other realistic features to develop. The model is forced by annual mean winds (Hellerman and Rosenstien, 1983). These are built up linearly during the third year of the run from zero to their steady value.

During the first few days of the integration, large-scale barotropic Rossby waves are observed, but by day ten the main feature of the flow is a rudimentary Circumpolar Current, whose amplitude, measured by the transport through Drake Passage, grows roughly linearly with time. After 3 years, the transport is 150×10^6 m^3s^{-1}. When the winds are added, the model again responds in less than 10 days, by increasing the rate of change of the transport. At the end of the third year, when the wind forcing steadies, the transport is 180×10^6 m^3s^{-1}, about 23×10^6 m^3s^{-1}

larger than predicted by extrapolating the transport calculated before the winds were added. Between years five and six the transport, the total kinetic energy of the model and other diagnostics settle down, indicating that the momentum budget of the model is near its asymptotic state.

At the end of 6 years, the total Drake Passage transport is 195 x 10^6 m^3s^{-1} (Fig. 1). This is larger than the observed (Whitworth et al. 1982) value of 130 x 10^6 m^3s^{-1}. The baroclinic component of the transport, which is determined primarily by the north-south density gradient, is very similar to that observed. The difference in barotropic transport can be accounted for by an excess eastward bottom velocity of 0.021 ms^{-1}. The velocity field in the Passage has a banded structure (Fig. 2) similar to that observed experimentally (Whitworth et al. 1982). Here, as elsewhere, the model sharpens the Levitus temperature field to produce a series of fronts (Fig.3). In the Passage, three of these correspond to eastward jets. A well-defined Polar Front is found at 63°S, and a strong Subantarctic Front at 57.5°S. In between, a weaker front is observed, together with a recirculation feature, containing the only region of westward currents. (The two main fronts are also reproduced in the global model of Semtner and Chervin (1988) which has a resolution of 0.5° in the north-south direction and 20 levels in the vertical). Note that although the current structure near the fronts is predominantly baroclinic, there is a significant barotropic component. Away from the Drake Passage, the bottom velocity is almost everywhere eastward, in contradiction to a recent inverse calculation (Olbers and Wentzel, 1990).

Analysis of the stream function (Fig. 1) shows that topographic features dominate the path of the Circumpolar Current. In the S. Pacific the model shows that the current crosses the isolated Pacific-Antarctic ridge through the Menard, Eltanin and Udintsev fracture zones. The maximum flow is found at the southernmost Udintsev fracture zone where the current has a total transport of 100 x 10^6 m^3s^{-1} through a channel less than 130 kms wide. On each side of the region steering by the topography is evident. In addition, strong eddy activity is observed near the ridge axis, with less visible on the neighbouring abyssal plains. This is in qualitative agreement with the GEOSAT observations of surface variability (Chelton et al. 1990).

The distribution of current speeds (Fig. 4) shows narrow bands of strong currents (above 0.3 ms^{-1}). These are generally associated with strong topographic features in the path of the current. To the east of Drake Passage, one such feature is the Falkland Current, which plays the role of a western boundary current as the axis of the Circumpolar Current shifts from 60°S to 45°S. Other current bands may be distinguished near Kerguelen and south of the Campbell Plateau off New Zealand. The transport of the Falkland Current is 67 x 10^6 m^3s^{-1} at 48°S and 42 x 10^6 m^3s^{-1} at 44°S. (Observations (Stramma 1989) of just the baroclinic part of the flow give 10 x 10^6 m^3s^{-1} at 46°S).

The Brazil Current has a barotropic flux of 26 x 10^6 m^3s^{-1} at 33°S (17.5 x 10^6 m^3s^{-1} is observed (Gordon and Greengrove, 1986)), increasing to 30 x 10^6 m^3s^{-1} in the recirculation region at 35°S. The model shows the current separating from the coast at this latitude, in good agreement with observations. The East Australian Current has a flux of 37 x 10^6 m^3s^{-1} at 30°S. This is slightly higher than observed, possibly the result of the neglect by the model of the Pacific-Indian Ocean throughflow north of Australia. The current separates from the coast at 32°S, and generates a series of eddies which drift southwards, in good agreement with observations (Boland and Hamon 1970).

The most eddy-energetic region is the Agulhas Current off S. Africa. In the north, its transport is 57 x 10^6 m^3s^{-1} at 30°S. This compares favourably with observations (Toole and Raymer 1985, Gründlingh 1980) of 44 x 10^6 m^3s^{-1} to 60 x 10^6 m^3s^{-1}. The flux increases to 89 x 10^6 m^3s^{-1} at 35°S at the start of the recirculation region. During the spinup of the model, eddies were not formed until the transport in the Agulhas Current exceeded 50 x 10^6 m^3s^{-1}. During the later part of the spinup, a new eddy formed roughly every 160 days and drifted into the S. Atlantic with a speed of 0.04 ms^{-1}. At the moment of separation, the total transport around an eddy is 130 x 10^6 m^3s^{-1}.

The total heat content of an eddy relative to its surroundings is 2.6 x 10^{21} Joules and its volume is about 1.4 x 10^{14} m^3. This yields a total heat flux from the Indian to Atlantic Oceans due to the eddies of around 0.2 PW and a mass flux of 10 x 10^6 m^3s^{-1}.

These Agulhas eddies decay rapidly once in the S. Atlantic, the e-folding time of the total transport within each eddy being less than one year. This is more rapid than the expected lateral diffusion time of three years, and is almost certainly due to the relaxation to Levitus used in this part of the model run. Further south, we find that the eddies generated by the Circumpolar Current propagate only short distances, again probably due to the imposed relaxation. (The decay was much reduced when the run was continued with the relaxation removed.)

South of the Circumpolar Current, the main feature is the Weddell Gyre, with a total transport of 26 x 10^6 m^3s^{-1}. The model shows that it extends eastwards as far as the Kerguelen Plateau. The Ross Sea also forms a cyclonic gyre, with a transport of 7 x 10^6 m^3s^{-1}, extending from 160°E to 140°W.

The only serious numerical problem found with the model is an up to 2 x 10^6 m^3s^{-1} plus-minus feature evident in parts of the stream function. This produces blue-weighted noise in the barotropic velocity with an amplitude of about 0.01 ms^{-1}. Later parts of the run will include biharmonic viscosity to reduce this error.

The present model has shown that by going to an eddy resolving scale, a significant improvement in the performance of ocean models can be achieved. Some of the important processes involved in climate change, such as deep convection at high latitudes, may still not be resolved adequately but the results represent a significant improvement over those of non-eddy resolving models.

ACKNOWLEDGMENTS

The FRAM Community Research Project is supported by the Natural Environment Research Council. Computations were performed at the Atlas Computer Laboratory. Valuable graphical work was provided by Andrew Anson, Jeffrey Blundell, and Tim Hateley.

REFERENCES

BOLAND, F.M. & HAMON, B.V. 1970. The east Australian Current, 1965-1968.
Deep-Sea Research, 17, 777-794.

CHELTON, D.B., SCHLAX, M.G., WITTER, D.L. & RICHMAN, J.G. 1990. Geosat altimeter observations of the surface circulation of the Southern Ocean.
Journal of Geophysical Research, 95, 17877-17903.

COX, M.D. 1984. A primitive equation, 3-dimensional model of the ocean.
Geophysical Fluid Dynamics Laboratory Ocean Group Technical Report, No.1.

DBDB5 data set, U.S. Naval Oceanographic Office.

GORDON, A.L. & GREENGROVE, C.L. 1986. Abyssal eddy in the south-west Atlantic.
Deep-Sea Research, 33, 839-847.

GRÜNDLINGH, M.L. 1980. On the volume transport of the Agulhas Current.
Deep-Sea Research, 27, 557-563.

HELLERMAN, S. & ROSENSTEIN, M. 1983. Normal monthly wind stress over the world ocean with error estimates.
Journal of Physical Oceanography, 13, 1093-1104.

KILLWORTH, P.D. 1987. Topographic instabilities in level model OGCMs.
Ocean Modelling, 75, 9-12.

LEVITUS, S. 1982. Climatological Atlas of the World Ocean.
NOAA Professional Paper, No.13. 173pp.

OLBERS, D. & WENTZEL, M. 1990. Determining diffusivities from hydrographic data by inverse methods with applications to the Circumpolar Current.
pp 95-139 in, Oceanic circulation models: combining data and dynamics (eds. D.L.T. Anderson & J. Willebrand)
Dordrecht: Kluwer Academic Publishers, 605pp.

SARMIENTO, J.L. & BRYAN, K. 1982. An ocean transport model for the North Atlantic.
Journal of Geophysical Research, 87, 394-408.

SEMTNER, A.J. & CHERVIN, R.M. 1988. A simulation of the global ocean circulation with resolved eddies.
Journal of Geophysical Research, 93, 15502-15522.

STEVENS, D.P. 1990. On open boundary conditions for three dimensional primitive equation ocean circulation models.
Geophysical and Astrophysical Fluid Dynamics, 51(1-4), 103-133.

STRAMMA, L. 1989. The Brazil Current transport south of 23S.
Deep-Sea Research, 36, 639-646.

TOOLE, J.M. & RAYMER, M.E. 1985. Heat and fresh water budgets of the Indian Ocean - revisited.
Deep-Sea Research, 32, 917-928.

WHITWORTH, T., NOWLIN, W.D. & WORLEY, S.J. 1982. The net transport of the Antarctic Circumpolar Current through Drake Passage.
Journal of Physical Oceanography, 12, 960-971.

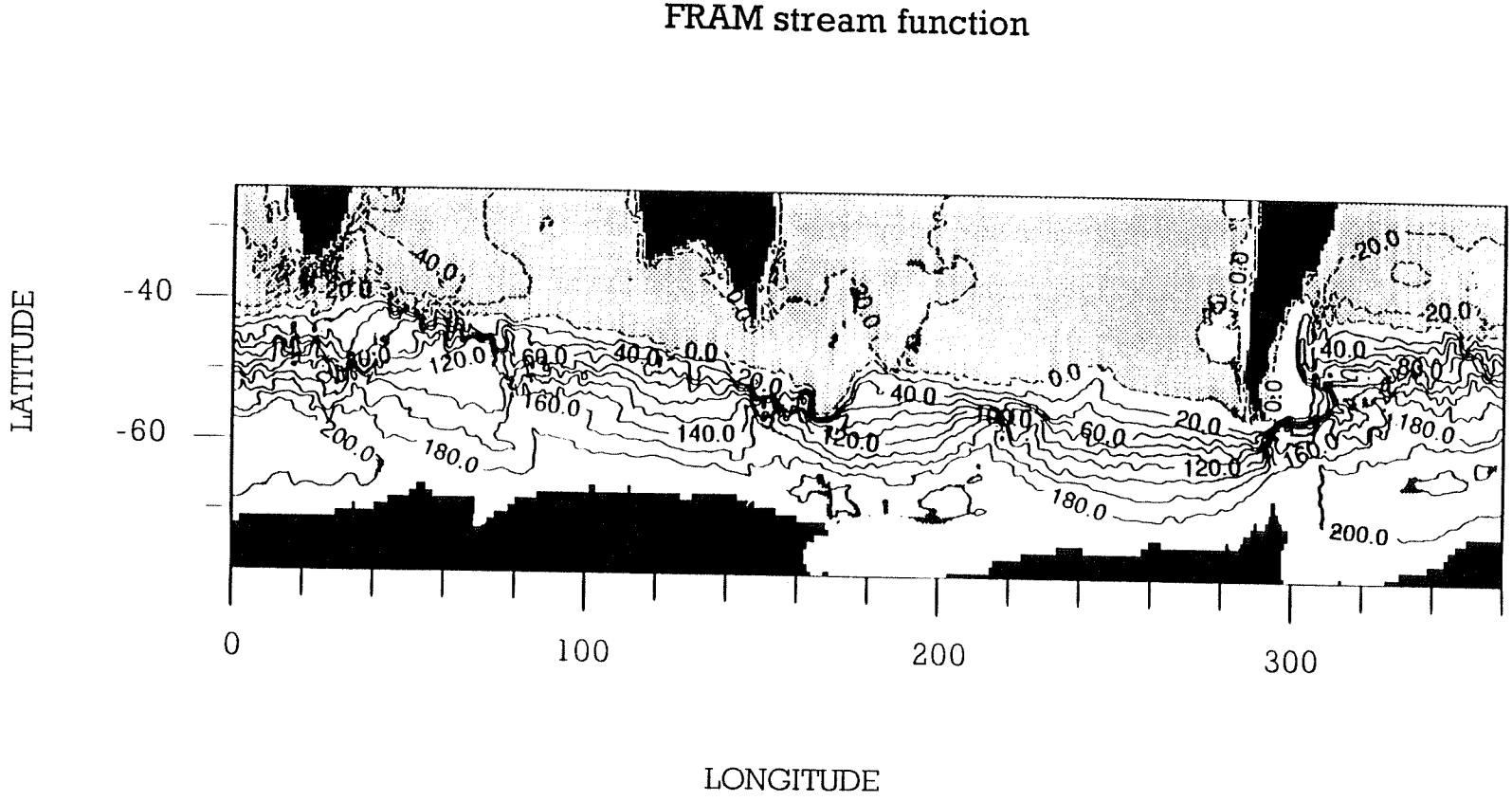

Figure 1. Contours of stream function (depth integrated transport) in units of 10^6 m^3s^{-1} at the end of six years. Contour interval 20; negative values shaded.

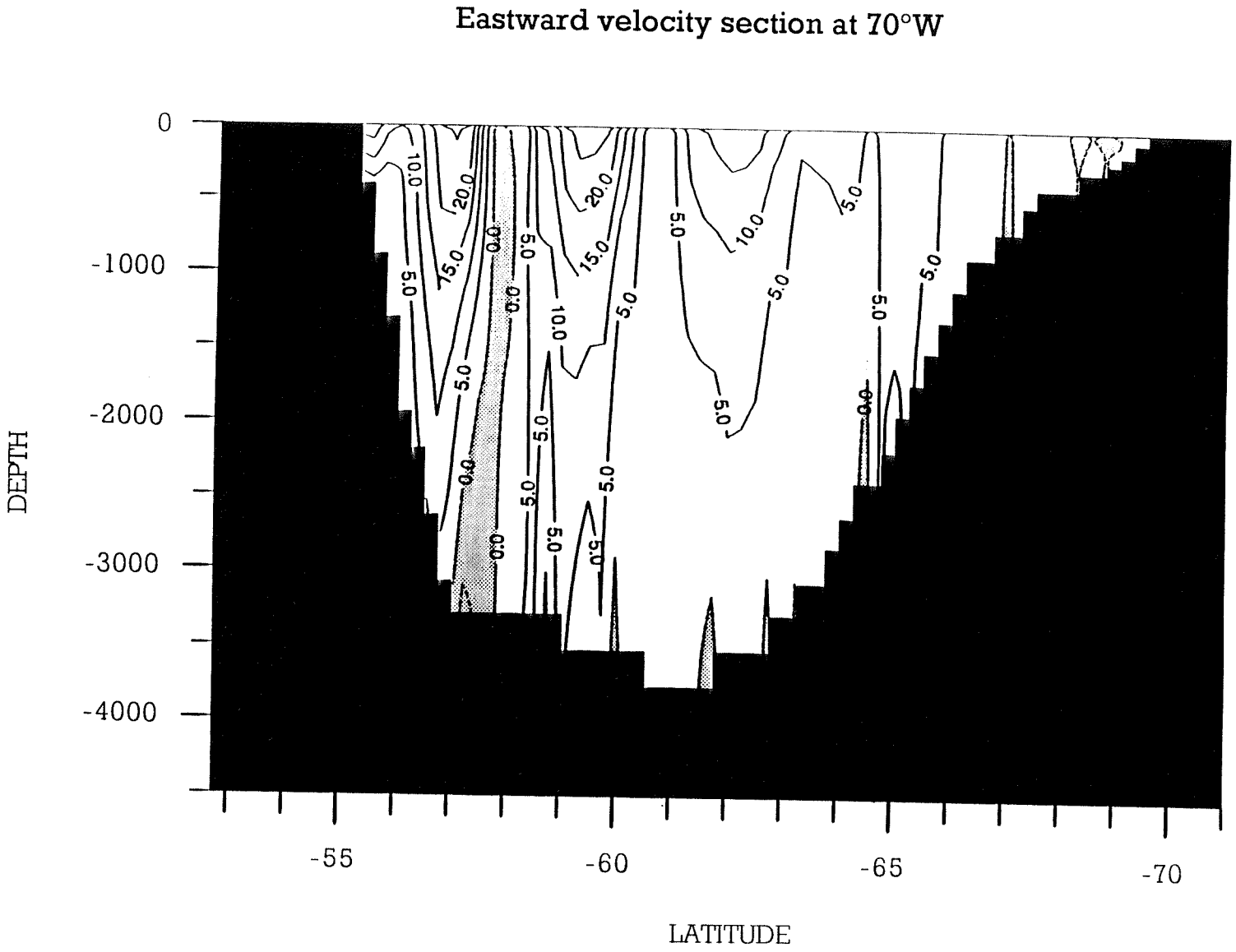

Figure 2. Contours of eastward velocity on a north-south section across the Drake Passage at 70°W at the end of six years. Contour interval 5 cms^{-1}; negative values shaded. (Maximum 30.0 cms^{-1}, minimum -6.7 cms^{-1}.)

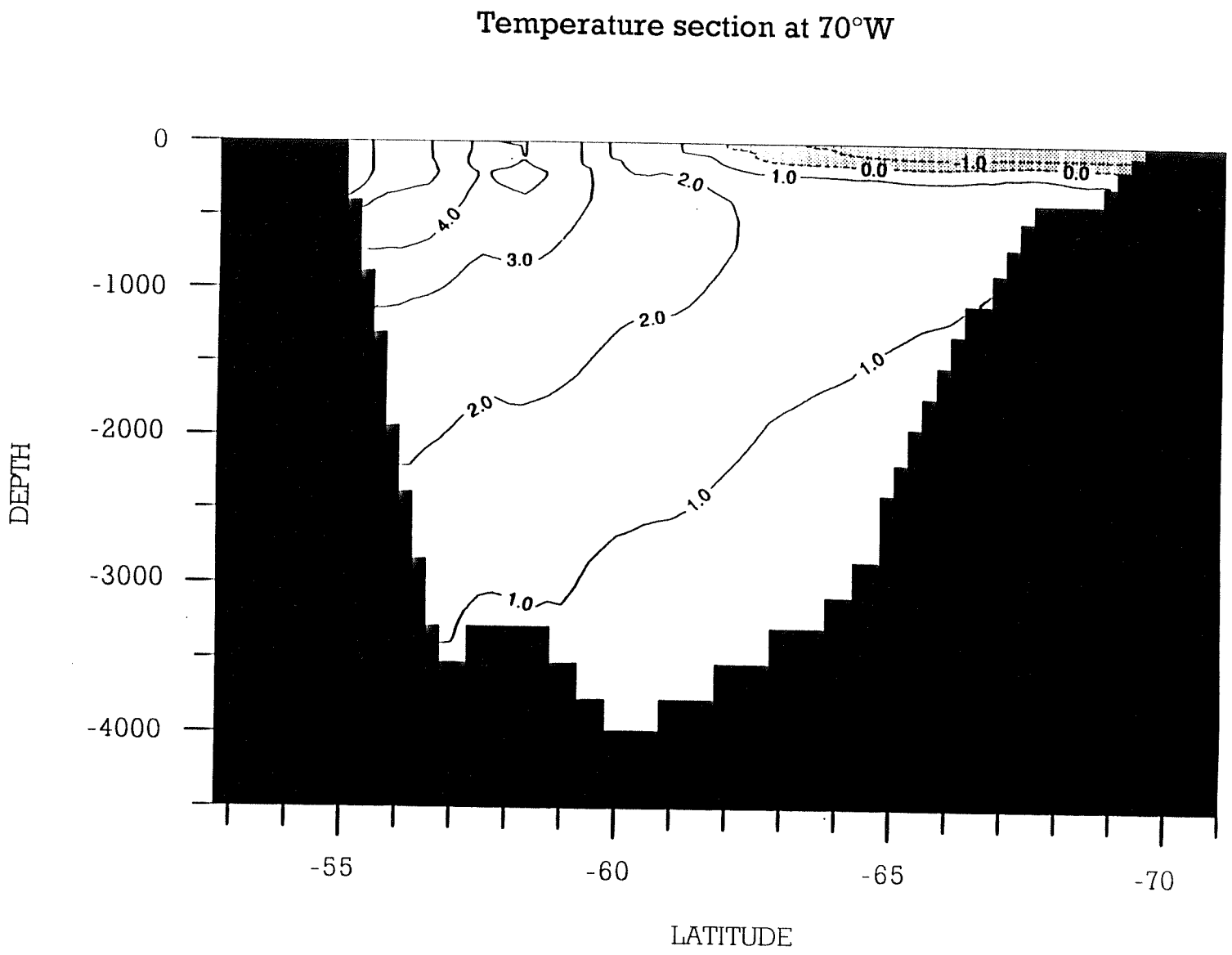

Figure 3. Contours of temperature on a north-south section across the Drake Passage at 70°W at the end of six years. Contour interval 1°C; negative values shaded. (Maximum 6.9°C, minimum -1.4°C.)

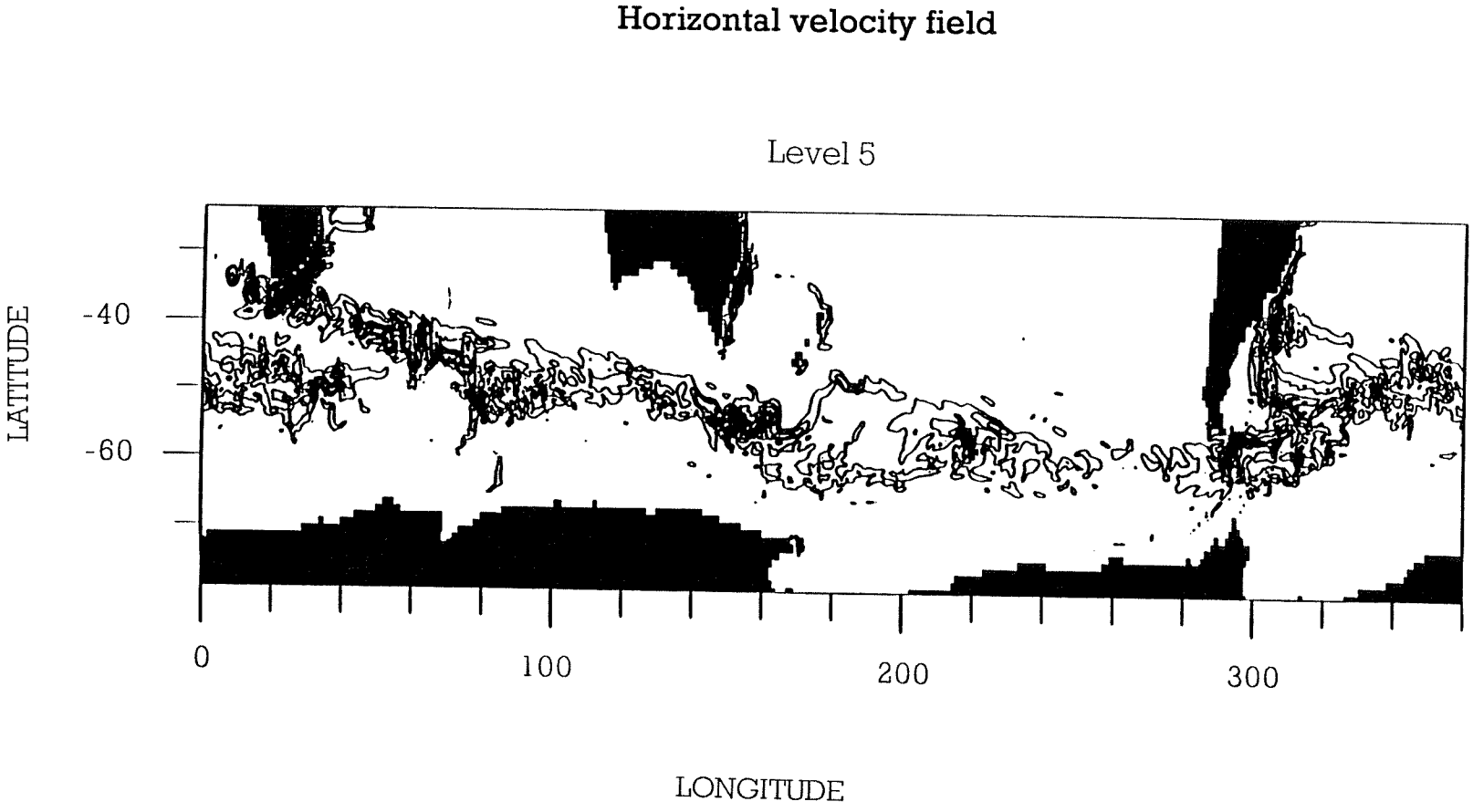

Figure 4. Contours of current speed at 100 m depth at the end of six years. Contour interval 0.1 ms^{-1} (maximum speed 1.5 ms^{-1}).